J Food Sci Technol (January 2020) 57(1):152–162
https://doi.org/10.1007/s13197-019-04041-9

ORIGINAL ARTICLE

Insoluble dietary fiber from soy hulls regulates the gut microbiota in vitro and increases the abundance of bifidobacteriales and lactobacillales

Lina Yang[1,2,3] · Yafan Zhao[1,3] · Jinghang Huang[1,3] · Hongyun Zhang[1,3] · Qian Lin[1,3] · Lin Han[1,3] · Jie Liu[2] · Jing Wang[2] · He Liu[1,3]

Revised: 14 August 2019 / Accepted: 19 August 2019 / Published online: 23 August 2019

Abstract We evaluated soy hull dietary fibers (SHDF) extracted from different raw materials, in terms of their chemical composition, physicochemical properties, structure, and ability to regulate fecal microflora, in order to investigate the properties and functions of SHDF. The structures of insoluble dietary fiber from soy hull with oxalic acid extraction (IDFO) and insoluble dietary fiber from soy hull with citric acid extraction (IDFC) were characterized by scanning electron microscopy, Fourier transform infrared spectroscopy, and X-ray diffraction. Compared with IDFO, IDFC had larger crystalline regions, and a higher water retention capacity (4.92 g/g), water swelling capacity (4.77 mL/g), oil adsorption capacity (1.60%), α-amylase activity inhibition ratio (12.72%), glucose adsorption capacity (1.59–13.42%), and bile acid retardation index (5.18–26.61%). Given that the gut microbiota plays a pivotal role in health homeostasis, we performed a detailed investigation of the effects of dietary fiber on fecal microbiota through 16S rDNA high-throughput sequencing. As revealed by Venn, principal component analysis, and 3D-principal co-ordinates analysis analysis, the structure of the fecal microbiota community was markedly altered by intake of IDFO and IDFC. In particular, the abundance of Bifidobacteriales and Lactobacillales significantly increased to varying degrees as a result of IDFO and IDFC intake. Altogether, this study demonstrates a prebiotic effect of SHDF on the fecal microbiota in vitro and provides a basis for the development of SHDF as a novel gut microbiota modulator for health promotion.

Keywords Dietary fiber · Structure · Functional property · Gut microbiota

✉ He Liu
liuhe2069@163.com

[1] College of Food Science and Technology, Bohai University, Jinzhou 121013, Liaoning, China

[2] China-Canada Joint Lab of Food Nutrition and Health (Beijing), Beijing Technology and Business University, Beijing 100048, China

[3] National and Local Joint Engineering Research Center of Storage, Processing and Safety Control Technology for Fresh Agricultural and Aquatic Products, Jinzhou 121013, Liaoning, China

Introduction

In recent years, dietary fiber has gradually become known as one of the seven major classes of nutrients for humans. In 2009, the Codex Alimentarius Commission defined dietary fiber (DF) (McCleary et al. 2013) as being formed from carbohydrate polymers with ten or more monomeric units that cannot be hydrolyzed by enzymes in the human small intestine. DF includes edible carbohydrate aggregates present in the food itself, as well as carbohydrate polymers derived from food materials through physical, enzymatic, or chemical methods, or synthetic polymers that are beneficial for health. In general, DF is divided into soluble dietary fiber (SDF) and insoluble dietary fiber (IDF). SDF includes β-glucan, galactomannan, pectin, psyllium, inulin, and resistant starch, whereas IDF includes cellulose, hemicellulose, chitosan, lignin, etc. Previously, SDF was considered to decrease serum lipid and glucose levels, whereas the effect of IDF was mainly thought to be fecal bulking (Kaczmarczyk et al. 2012). Subsequently, increasing evidence has revealed the relationship between IDF and health. For instance, IDF results in lower weight gain, improved insulin sensitivity (Weickert et al. 2011),

lowered blood pressure, and improved immune function (Aljuraiban et al. 2015). Fecal dilatation and shorter intestinal transit time can prevent constipation and may dilute or decrease the absorption of toxic or carcinogenic metabolites, thereby improving gastrointestinal health and decreasing the risk of tumor development and cancer. In spite of previous research efforts, however, whether and, if so, how IDF affects the gut microbiota is largely unknown.

The gut microbiota has recently become a new focus of research at the intersection between diet and metabolic health (Gong et al. 2018a, b). High fiber diets provide an abundant supply of fermentable substrate for the gut microbiota, which modulates the systemic health of the host through direct and indirect effects. These effects are due to IDFs being little absorbed and thus interacting with the gut microbiota for a long time in the intestinal tract. The gut microbiota is greatly influenced by the fermentability of ingested fibers; consequently, the gut microbiota may link IDF and human health. With the development of high-throughput sequencing technology and metagenomics, increasing evidence has identified the role of the gut microbiota in the etiology of host chronic metabolic diseases. Sun et al. (2019) found that oral treatment with water-insoluble polysaccharide significantly improved glucose and lipid metabolism in ob/ob mice (8 weeks old, obesity and type 2 diabetes in animal models) and decreased hepatic steatosis, as a result of an increase in the butyrate-producing bacteria of the Lachnospiraceae family, including *Clostridium*. Hashemi showed that pea seed coating increased the abundance of bacteria of the families the Lachnospiraceae and the Prevotellaceae in glucose-tolerant rats. In addition, cooked pea seed coating increased glucose tolerance by approximately 30%, whereas dietary raw and cooked pea seed coating was found to decrease the insulin response by 53% and 56%, respectively (Hashemi et al. 2017). Velikonja performed a double-blind, placebo-controlled, randomized clinical trial of 43 volunteers diagnosed with metabolic syndrome or high-risk of progression to metabolic syndrome. In a four-week intervention study, participants consumed experimental bread containing 6 g of barley beta glucan (BBG) or the same bread without beta glucan. Abundance of the Coriobacteriales was significantly reduced, and that of the Coriobacteriales species *Collinsella aerofaciens*, which is associated with colorectal cancer and thrives in an inflamed intestinal environment, showed a decreasing trend following BGB intervention (Velikonja et al. 2019). These results highlight the possible positive effects of beta glucan on host health and support its prebiotic effect.

Soybean is the most important source of edible plant oil and protein worldwide. Thousands of tons of soy hulls and dregs are generated as agricultural by-products and are typically discarded and wasted. Soy hulls are a good source of IDF, and thus their utilization may benefit human health and the protection of the environment. The objective of this study was to evaluate the functional effects on the gut microbiota of different IDFs extracted from soy hulls. The physicochemical properties and structure of IDF were first determined. After potential differences in IDFs were identified, the changes in the profiles of the gut microbiota were further analyzed by 16S rDNA high-throughput amplicon sequencing. The findings of this study should provide useful insights into the potential applications of DF from soy hull by-products.

Materials and methods

Structural characterization

Scanning electron microscopy (SEM)

The surface and microstructure of DFs were observed by SEM (S-4800 scanning electron microscope, Japan) at 3.0 kV. The dry samples were placed on a metal disk with double-faced conducting adhesive tape and coated with a gold layer of 10 nm. Representative micrographs were taken for each sample at 1000× magnification.

Fourier-transform infrared spectroscopy (FTIR)

DFs were thoroughly mixed with KBr (1:150, w/w) and pelletized. IR spectra of the IDFO and IDFC were recorded on a FTIR-650 spectrometer (Thermo Nicolet Corporation, USA) from 400 to 4000 cm^{-1} with 32 scans and a resolution of 4 cm^{-1}.

X-ray diffraction (XRD)

X-ray diffraction (XRD) analysis of the dry sample was carried out according to Wen et al. (2017), with slight changes. The XRD pattern was determined in an X-ray powder diffractometer (Bigaku Ultima IV, Japan) using Cu radiation at 40 kV and an incident current of 40 mA. The angular region was scanned in the range of 5° to 70° with a step length of 0.02 and a step rate of 10°/min.

DF preparation and physicochemical properties

The method of extracting dietary fiber (DF) from soy hulls by enzymes was modified according to Ma et al. (2015), and the soy hull dregs, after microwave assisted extraction of the soluble polysaccharides using oxalic acid and citric acid, were mixed with deionized water at a 1:10 ratio and hydrolyzed with alkaline protease (Yuanye, Shanghai,

China) (200 U/mg) at 55 °C for 155 min. After the reaction, the mixture was heated in a boiling water bath for 15 min to terminate the hydrolysis, then centrifuged at 4000 rpm for 20 min and dried at 65 °C to constant weight.

Water retention capacity (WRC) was determined according to the method reported by López-Marcos et al. (2015). DFs (1 g) were hydrated in a centrifuge tube with 30 mL deionized water at room temperature for 18 h, and the supernatant was removed after centrifugation at 4000 rpm for 20 min. WRC was calculated according to the weight of the resulting residue recorded both before and after drying at 105 °C to constant weight, with the following equation:

$$\mathrm{WRC\,(g/g)} = \left(m_f - m_d\right) - m_d$$

where m_f is the weight of hydrated residue (g), and m_d is the weight of dried sample (g).

The water swelling capacity (WSC) was determined according to the method reported by Sowbhagya et al. (2007). DFs (0.2 g) were hydrated in 10 mL deionized water in a graduated test tube at room temperature for 18 h, and the volume of dietary fiber was calculated after water absorption. WSC was determined by the following equation:

$$\mathrm{WSC\,(mL/g)} = (v_1 - v_0)/w_0$$

where v_1 is the volume of the hydrated sample, v_0 is the volume of the dried sample, and w_0 is the weight of the dried sample.

The oil adsorption capacity (OAC) was determined through the method described by López-Marcos et al. (2015), with slight modifications. DFs (0.2 g) were mixed with 30 mL corn oil for 18 h at room temperature. The supernatant was removed after centrifugation at 4000 rpm for 20 min and the residue weighed. OAC was determined by the following equation:

$$\mathrm{OAC\,(g/g)} = (m_r - m_d) \times 100/m_d$$

where m_r is the residue weight, which contained the oil (g), and m_d is the original weight of DF (g).

Functional properties

Glucose adsorption capacity (GAC) was determined by the method described by Luo et al. (2018). Each sample (1 g) was mixed with 100 mL of glucose at different concentrations (50, 100, and 200 mmol/L) and incubated in a water bath at 37 °C for 6 h. After the glucose adsorption had reached its equilibrium, samples were centrifuged at 4000 rpm for 20 min, and the glucose concentration in the supernatant was measured with a glucose assay kit (Yuanye, Shanghai, China). GAC was calculated according to the following equation:

$$\mathrm{GAC\,(mmol/g)} = C_i - C_s \times V_i/W_s$$

where C_i is the glucose concentration of the original solution (mmol/L), C_s is the supernatant glucose content when adsorption reached equilibrium (mmol/L), W_s is the weight of DF (g), and V_i is the supernatant volume (mL).

The α-amylase activity inhibition ratio (α-AAIR) was determined with the method described by Ahmed et al. (2011). A 4% (w/v) starch solution was prepared as follows: potato starch (4 g) and 90 mL 0.05 mol/L phosphate buffer (pH6.5) were mixed at 65 °C for 30 min, and the volume was adjusted to 100 mL with phosphate buffer (pH6.5). A starch-α-amylase-DF system consisting of the above starch solution (25 mL), α-amylase (Yuanye, Shanghai, China) (0.4%), and tested DF (1%) was dialyzed (SP132703: 12,000–14,000; Yuanye, China) against 200 mL of deionized water (pH 7.0) at 37 °C for 60 min in a shaking water bath. Then, the glucose concentration of the dialysate was measured with a glucose assay kit (Yuanye, Shanghai, China). A control test was carried out without DF, and α-AAIR was calculated from the following equation:

$$\alpha - \mathrm{AAIR}(\%) = (A_C - A_S) \times 100/A_C$$

where A_C is the absorbance of the control, and A_S is the absorbance of DF.

The bile acid retardation index (BRI) was determined through the method described by Ma and Mu (2016), with slight modifications. 15 mmol/L of taurocholic acid sodium salt solution was prepared with 0.05 mol/L phosphate buffer at pH 7. DF (0.2 g) was mixed with the sodium taurocholate solution and transferred into a dialysis membrane (SP132703: 12,000–14,000; Yuanye, Shanghai, China). The dialysis bag was placed in 100 mL of phosphate buffer (pH 7) at 37 °C. Sodium taurocholate without DF was used as the control. An aliquot (2 mL) of the dialyzate was removed for analysis at 60 and 120 min, and the concentration of sodium taurocholate was measured by HPLC (Agilent 1260, Agilent, USA). Briefly, the dialyzed taurocholic acid solution was filtered before being injected onto a Symmetry C18 (Agilent, USA) (4.6 mm 250 mm) HPLC column with acetonitrile (Reagent A) and disodium hydrogen phosphate (0.15%, pH 3.0, Reagent B) as mobile phases. The mobile phase linear gradient consisted of 22–42% A for 30 min followed by 42–35% A for 5 min. The flow rate was 1.0 mL/min. A UV detector at 203 nm was used to detect taurocholic acid. BRI was calculated with the following equation:

$$\mathrm{BRI\,(\%)} = 100 - [(C_d \times 100)/C_c]$$

where C_d is the total taurocholic acid concentration diffused from the DF (mmol/L), and C_c is the total taurocholic acid concentration diffused from the control (mmol/L).

In vitro fermentation culture

Sugar-free medium was prepared, containing 2.25 g/L yeast extract, 0.75 g/L tryptone, 3.0 g/L mucoprotein, 0.37 g/L L-cysteine, 12.5 g/L NaCl, 6.0 g/L bile salt and 0.9 g/L pancreatin, according to Truchado et al. (2017). IDFO and IDFC and control glucose were added at a concentration of 1%. Fresh feces were mixed in equal proportions from three healthy volunteer without any gastrointestinal diseases and antibiotic therapy in the past half year and added to a sterile 0.01 mol/L phosphate-buffered solution pH at 7.4 to prepare a stool slurry, which was added to the culture system at a ratio of 1:10 and cultured at 37 °C for 48 h in an anaerobic incubator (90% N_2, 5% H_2 and 5% CO_2) (LAI-3, Shanghai Longyue Instrument Equipment Co., Ltd. China) (Strain et al. 2019). The DNA of original and cultured fecal microbiota (FM) was extracted according to manufacturer's instructions QIAamp Fast DNA Stool Mini Kit (QIAGEN, Germany). The V3–V4 region of the 16S rDNA gene fragments was amplified using a set of primer pairs (341F; 5′-CCCTACACGAC GCTCTTCCGATCTG (barcode) CCTACGGGNGGC WG CAG-3′, 805R; 5′-GACTGGAGTTCCTTGGCACCCGAG AATTCCAGACTACHVGGGTATCTAATCC -3′). Statistical analysis of biological information is typically performed at OTUs at 97% similar levels. The abundance and diversity of environmental communities were estimated using statistical analysis indexes such as Chao, Ace, Shannon, and Simpson. Principal component analysis (PCA) of OTU in different samples was performed to compare the structure of the microbiota between samples. The differences between the samples were observed by UniFrac-PCoA.

Statistical analyses

All experiments were performed with three replicates, and the data are expressed as mean ± standard deviation. Data were analyzed using the statistical analysis software SPSS Statistics 19.0 (IBM, Armonk, NY, USA). Results were considered to be statistically significant at $p < 0.05$.

Results and discussion

Structural characterization

Scanning electron microscopy (SEM)

The morphologies of IDFO and IDFC after enzymatic hydrolysis by protease are depicted in Fig. 1a. The SEM images showed that the morphology of IDFO included a compact regularly folded surface with visible attached particles and spherical substances, which might have been residual starch granules. Wen et al. (2017) also found similar results. IDFC formed a loose structure with a smooth surface, and the inner structure had holes exposed. Alterations in the internal and external structure of IDFC allowed more water molecules to participate in hydrogen bonding and/or dipole formation, and hence may have improved its water retention capacity and swelling capacity (Chen et al. 2014).

Fourier-transform infrared spectroscopy (FTIR)

Figure 1b shows the FTIR spectrum of IDFO and IDFC from 400 to 4000 cm^{-1}. The spectroscopic profiles of most bands of IDFO were comparable to those observed in IDFC, indicating similarities in the chemical functional groups of the two samples. It can be seen from Fig. 1b that the infrared images of IDFO and IDFC have no difference and have the same functional groups. There was a broad band at 3421 cm^{-1} assigned to O–H stretching of hydrogen combined with hydroxyl groups mainly derived from cellulose and hemicellulose (Xiao et al. 2017). The peak at 2920 cm^{-1} indicated the presence of the C–H vibration of the saccharide methylene group. The significant peaks observed at 1735 cm^{-1} and 1618 cm^{-1} were due to hemicellulose-specific acetyl or C=O bonds, as well as methyl esterification or free carboxyl groups specific for pectin (Kaushik and Singh 2011). The broad peaks at 1430–1320 cm^{-1} and the nearby shoulder peak corresponded to the stretching vibration of the C–O bond in COOR. The peak at 1155 cm^{-1} was ascribed to C–O–C stretching vibration of hemicellulose and cellulose, and that at 1060 cm^{-1} was indicative of stretching vibration of C–O in hemicellulose and cellulose (Bibin Mathew et al. 2008), in agreement with the structure of cellulose. There were three peaks at 1100–1010 cm^{-1}; the characteristic absorption peak of pyranoside, whereas the furanoside had two peaks in this region. β-type pyranose has a peak at 891 ± 7 cm^{-1}. A peak at 896 was indicative of stretching vibration of β-pyranose and C–H variable angle vibration (Fig. 1b) (Liu et al. 2014).

X-ray diffraction (XRD)

The XRD patterns and changes in the crystallinity of IDFO and IDFC were investigated. As shown in Fig. 1c, distinct diffraction peaks were observed at 2θ angles of 22.26° and 34.5°, representing a typical crystalline cellulose I structure (Wen et al. 2017). IDFO had a sharp peak at 14.88, whereas IDFC had a wider peak. Cellulose consists of linear chains of β (1–4) linked D-glucopyranose units that aggregate and form the core of crystalline cellulose. The crystalline portion was indicated by the sharp peak in the

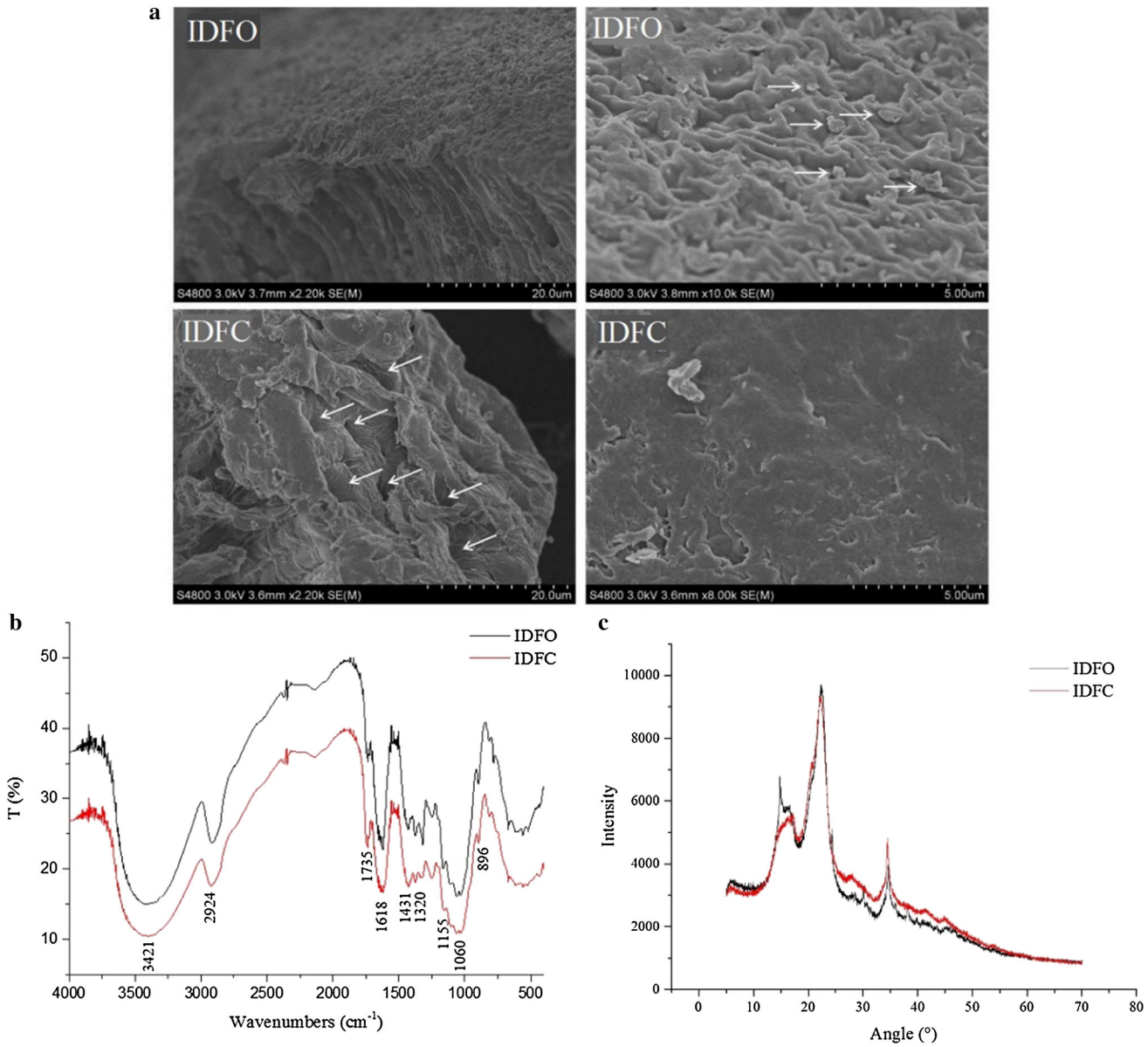

Fig. 1 Scanning electron microscopy (SEM) (**a**), Fourier-transformed infrared spectroscope (FTIR) spectra (**b**), and X-ray diffraction (XRD) patterns (**c**) of IDFO and IDFC. IDFO, insoluble dietary fiber from soy hull with oxalic acid extraction; *IDFC* insoluble dietary fiber from soy hull with citric acid extraction

picture, and an amorphous portion was also observed (Nishiyama et al. 2003). Hemicellulose is generally linked with cellulose microfibers but has a random, amorphous structure with little strength, which can be easily hydrolyzed by various hemicellulases (Scheller and Ulvskov 2010). It can be seen from Fig. 1c that the amorphous peak is at 17.8°. The difference between IDFO and IDFC is that IDFO has a sharp peak at 14.88°. The reason may be that the oxalic acid has a lower pH than citric acid in the pretreatment of the raw material, and enhanced the peak intensity.

Physicochemical properties

As shown in Table 1, analysis of two types of DF from soy hulls demonstrated comparable concentrations of moisture, fat, starch, and ash in the two samples. The IDF concentration of IDFO (82.78%) was significantly higher than that of IDFC (79.82%) ($p < 0.05$), whereas the SDF concentration of IDFC (6.41%) was significantly higher than that of IDFO (4.63%) ($p < 0.05$). In the study of Yang et al. (2014), the concentration of IDF and SDF in soy hulls processed with acid–base hydrolysis and high pressure was 86.5 g/100 g and 1.0 g/100 g. The IDF of IDFO and IDFC

Table 1 Proximate composition of IDFO and IDFC

DF	Moisture	Protein	Fat	Starch	Ash	IDF	SDF
IDFO	4.17 ± 0.28[a]	0.036 ± 0.0034[b]	1.23 ± 0.16[a]	3.78 ± 0.93[a]	2.36 ± 0.058[a]	82.78 ± 0.0067[a]	4.63 ± 0.0017[b]
IDFC	4.53 ± 0.17[a]	0.052 ± 0.00067[a]	0.92 ± 0.2[a]	3.89 ± 0.23[a]	2.42 ± 0.079[a]	79.82 ± 0.0033[b]	6.41 ± 0.0026[a]

Data are expressed as g/100 g dry basis except for moisture content. Values are mean ± SD, $N = 3$. Values with a different letter in the same column are significantly different, $p < 0.05$ (Student's t test). Error bar represents SD

IDFO insoluble dietary fiber from soy hull with oxalic acid extraction, *IDFC* insoluble dietary fiber from soy hull with citric acid extraction, *DF* dietary fiber, *IDF* insoluble dietary fiber, *SDF* soluble dietary fiber

was slightly lower than its IDF content, compared with Yang. The total DF concentration of soy hulls was higher than that reported in other cereals and fruits, including rice bran (27.04 g/100 g), sesame coat (31.64 g/100 g), peach DF concentrate (30.7 g/100 g), orange DF concentrate (36.9 g/100 g), and mango DF concentrate (28.05 g/100 g) (Abdul-Hamid and Yu 2000; Elleuch et al. 2010; Liu et al. 2018; Vergara-Valencia et al. 2007). The fiber concentration of okara IDF was 82.6 g/100 g. These findings indicate that soy hulls are an excellent source of DF, as a result of their high DF content (Ullah et al. 2018). The difference in protein between IDFO and IDFC may have been caused by different types of acid used in the pre-treatment of the soy hulls, which may have resulted in different effects on the structure of the protein, thus affecting the enzymatic hydrolysis effects of alkaline protease.

The physical and chemical properties of DF strongly affect the nutritive value and physiological functions of soybean foods. The WRC indicates the ability of DF to retain moisture when it is subjected to external forces such as centrifugal pressure, which can regulate the water distribution in the food system and has a strong effect on the appearance, flavor, and commercial value of food. The WRC of IDFO was 3.91 g/g, which was lower than that of the corresponding IDFC (4.92 g/g) (Table 2). In addition, the WRC of the IDFO and IDFC was higher than that of citrus fruits (1.65 g/g), bananas (1.71 g/g), apples (1.87 g/g), and grapefruits (2.09 g/g), but lower than that of coconut kernels (10.71 g/g) and mango peel (11.40 g/g) (Chau et al. 2007; Figuerola et al. 2005; Yalegama et al. 2013). These results may be attributed to the dependence of DF WRC on particle size, processing condition, and surface characteristics, such as porosity, charge density, surface, and microstructure (Chau et al. 2007). Moreover, the concentration of SDF may result in differences in WRC. The more SDF content represented the higher the WRC. The WRC value of IDF from bamboo shoot shell was 2.99 g/g, and this value significantly increased ($p < 0.05$) after enzymatic hydrolysis (4.96 g/g) and dynamic high pressure micro-fluidization treatment (8.27 g/g) (Luo et al. 2018).

The WSC is the ratio of the volume of the material immersed in excess water after DF equilibration to the actual weight of the DF. The WSC of IDFO (3.22 mL/g) was lower than that of IDFC (4.77 mL/g) (Table 2), possibly as a result of differences in the physical structure of DF. The IDFC showed a loose structure with many voids, as shown in the SEM image of IDFC (Fig. 1a); this structure facilitates the absorption of water. The WSC of unsieved deoiled cumin DFs obtained from enzymatic hydrolysis was 6.76 mL/g, a value higher than that of SHDF (Ma and Mu 2016).

The OAC indicates the ability of DF to absorb fat. As shown in Table 2, there was no significant difference between the OAC of IDFC (1.60 g/g) and IDFO (1.37 g/g). The OAC was related to the fat concentrations of DF, and the fat concentrations of IDFC and IDFO were similar, as shown in Table 1. The OAC values of IDFO and IDFC were higher than those of DFs extracted from grapefruits (1.20 g/g) and apples (0.60 g/g), but lower than those of DFs extracted from citrus fruits (1.81 g/g). In addition, the OAC depends on the surface characteristics of the fiber particles (Figuerola et al. 2005). The porosity of the DF was greater, and its ability to adsorb oil was stronger. The presence of pores in the SEM micrographs of IDFC is conducive to the adsorption of oil.

Functional properties

The GAC index indicates the ability of the DF to control postprandial blood glucose. Three different levels of glucose (50, 100, and 200 mmol/L) were used to assess the GAC of DF. As shown in Table 2, in general, the adsorption capacity of IDFC for glucose was stronger than that of IDFO, possibly as a result of the greater proportion of SDF in IDFC. SDF with higher viscosity could potentially enhance the entrapment of glucose molecules within the fiber network, thereby delaying glucose diffusion (Chau et al. 2007). The reticular structure of DF aids in glucose absorption and slows the diffusion of glucose molecules in the food system (Lecumberri et al. 2007). The glucose adsorption capacity is directly proportional to the molar

Table 2 Effects of extraction material on WRC, WSC, OAC, GAC, BRI, and α-AAIR of IDFO and IDFC

DF	WRC (g/g)	WSC (mL/g)	OAC (g/g)	GAC (mmol/g)			BRI (%)		α-AAIR (%)
				50 mmol/L	100 mmol/L	200 mmol/L	1 h	2 h	
IDFO	3.91 ± 0.019^{b}	3.22 ± 0.059^{b}	1.37 ± 0.042^{a}	1.58 ± 0.15^{a}	5.84 ± 0.48^{a}	13.02 ± 0.12^{b}	2.10 ± 0.44^{b}	8.98 ± 0.19^{b}	5.28 ± 1.29^{b}
IDFC	4.92 ± 0.073^{a}	4.77 ± 0.0095^{a}	1.60 ± 0.026^{a}	1.59 ± 0.088^{a}	5.88 ± 0.36^{a}	13.42 ± 0.11^{a}	5.18 ± 0.86^{a}	26.61 ± 0.23^{a}	12.72 ± 2.02^{a}

Values are mean ± SD of three determinations. Values with a different letter in the same column are significantly different, $p < 0.05$ (Student's *t* test)

DF dietary fiber, *IDFO* insoluble dietary fiber from soy hull with oxalic acid extraction, *IDFC* insoluble dietary fiber from soy hull with citric acid extraction, *WRC* water retention capacity, *WSC* water swelling capacity, *OAC* oil adsorption capacity, *GAC* glucose adsorption capacity, *BRI* bile acid retardation index, *α-AAIR* α-amylase activity inhibition ratio

concentration of glucose. Luo et al. (2018) has found that the GAC values of all insoluble DFs from bamboo shoot shell steadily increase with the increase of glucose concentration until the glucose concentration reaches 25 mM.

DFs with high BRI can effectively postpone or depress bile acid uptake during gastrointestinal digestion by accelerating the secretion of bile acids, thereby avoiding epithelial cell and DNA damage. The results showed that BRI increased with increasing dialysis time (Table 2). IDFC exhibited a higher BRI (8.98–26.61%) than did IDFO (2.10–5.18%). The BRI of deoiled cumin DF was 16.34–50.08% and increased with increasing dialysis time; in soy hulls, it was higher than those of IDFO and IDFC and exhibited the same change law (Ma et al. 2015).

DF suppresses the activity of α-amylase and improves the digestion characteristics of starch in food. The inhibition rate of α-amylase activity is related to its WRC and WSC. Higher WRC and WSC can decrease the fluidity of the system and the probability of collision between the enzyme and the substrate, thereby decreasing the enzymatic hydrolysis effect of α-amylase on starch. IDFC (12.72%) had a higher α-AAIR than did IDFO (5.28%). This result might be attributable to microstructure changes such as more porous fiber networks, which were induced by the particle size distribution; as shown as Fig. 1a, IDFC had more holes than IDFO. Therefore, a higher amount of α-amylase was adsorbed to DF, and a higher starch concentration was embedded in the porous fiber network. Overall, the functional characteristics of IDFC were stronger than those of IDFO.

Intake of DF changed the structure of the gut bacterial community

To adequately demonstrate the effect of DF on fecal microflora in vitro, we used high-throughput sequencing spanning the V3–V4 hypervariable regions of 16S rDNA. The chao1 index is commonly used in ecology to estimate the total number of species, and the Ace index is used to estimate the number of OTUs in a community. Alpha diversity refers to diversity within a particular region or ecosystem, often measured by species richness, as reflected by the Simpson and Shannon indices. It is commonly used in ecology to quantitatively describe the biodiversity of a region. The larger the Simpson index value, the lower the community diversity. The larger the Shannon value represented the higher the diversity of the community.

As shown in Table 3, IDFO and IDFC both induced detectable changes in community richness and diversity. Compared to the original FM, the Shannon indices responsive flora diversity shifted from 1.85 to 2.61 and 2.15, and the Simpson index changed from 0.39 to 0.15 and 0.25 in the IDFO and IDFC groups respectively with

Table 3 Diversity of fecal microbiota in DF-treated and control groups

Groups	Reads	OTUs	Coverage	Richness estimator		Diversity estimator	
				Ace	Chao1	Shannon	Simpson
IDFO	50,144	855	0.991524	1890.15	1388.14	2.61	0.15
IDFC	54,231	863	0.991149	2343.28	1572.63	2.15	0.25
GLU	50,569	352	0.996124	1029.64	660.23	1.07	0.58
FM	89,995	478	0.998433	609.65	552.21	1.85	0.39

IDFO insoluble dietary fiber from soy hull with oxalic acid extraction, *IDFC* insoluble dietary fiber from soy hull with citric acid extraction, *FM* fecal microflora, *GLU* glucose

the time of fermentation in vitro. However, the diversity of the GLU was reduced. These results indicated that the intake of DF increased the diversity of fecal microbiota. Compared with GLU, the increases in the OTUs and Ace and Chao1 indices in response to IDFO and IDFC indicated that the intake of DF increased the total number of fecal microbiota, and that IDFC was superior to IDFO in this respect. There was the same findings in other experiments Lam uses barley β-glucan as a raw material to explore its effects on infant feces. The study found that compared with glucose, the intake of barley β-glucan lead to the Shannon index and the Simpson reciprocal increased and showed significantly higher α-diversity (Lam et al. 2019). There are studies that show the high-throughput 16S rRNA amplicon sequencing are restricted to dominant bacterial populations, metagenomic and amplicon sequencing surveys report a number of approximately 150 dominant bacterial species detected per sample (Faith et al. 2013; Qin et al. 2010), whereas approximately 1000 bacterial species from the human intestine have been cultivated (Clavel et al. 2016; Rajilić-Stojanović and de Vos 2014). Therefore, IDFO and IDFC maybe induced more specific strains prolifration to increase the number of OUT in vitro.

We established a Venn diagram based on shared OTUs and performed principal component analysis (PCA) and 3D-principal coordinate analysis (3D-PCoA) (Fig. 2). The Venn diagram provided additional verification of our results, indicating the regulatory effect of DF on fecal microbiota, because the different groups had unique OTUs that were not shared with the negative controls (Fig. 2a). Moreover, as indicated in the PCA and 3D-PCoA score plots, the IDFC-treated group showed a much more significant structural shift than the IDFO-treated group, both along the first principal component and the second principal component (Fig. 2b, c). These results further demonstrated the significant differences in the effects of IDFC and IDFO on fecal microbiota. Shang has reported a modulatory effect of keratan sulfate on gut microbiota: different groups of treated mice had unique OTUs that were not shared with those of the negative controls. However, the amount of DFs added is an important factor in the regulation of the flora structure of intestinal microbes in vitro (Shang et al. 2016). Sasak found that 0.2% prebiotic intake had no effect on microbial composition. The PCoA of the unweighted UniFrac distance showed that the microbial population in the fecal sample followed the same direction as the corresponding culture without prebiotics ($p = 0.454$, multivariate analysis of variance) (Sasaki et al. 2018).

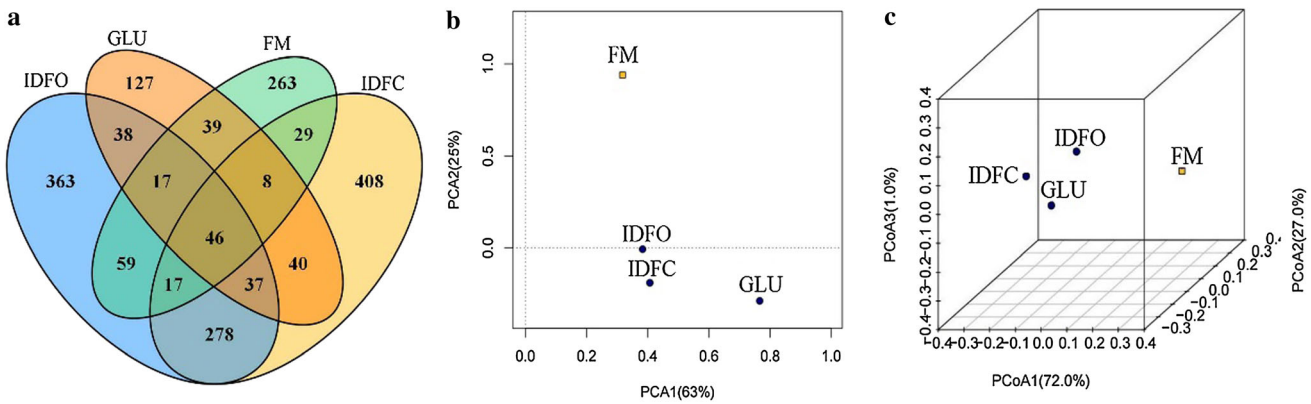

Fig. 2 Response of the fecal microbiota to DF treatment. Venn diagram representation of shared/unique OTUs in the fecal microbiota of IDFO, IDFC, and GLU treated and control groups (**a**). PCA score plot of the fecal microbiota in all groups (**b**). 3D-PCoA of the fecal microbiota in all groups (**c**). *IDFO* insoluble dietary fiber from soy hull with oxalic acid extraction, *IDFC* insoluble dietary fiber from soy hull with citric acid extraction, *FM* fecal microflora, *GLU* glucose

DF modulates the intestinal microbiota at different taxonomic levels

We compared the bacterial composition of the fecal microbiota at the phylum level and found that IDFO and IDFC significantly increased the abundance of Fusobacteria and Proteobacteria and decreased the population of Bacteroidetes and Firmicutes at the phylum level (Fig. 3a), with varying degrees of influence. We further compared the bacterial composition of the intestinal microbiota at the order level and found different effects of IDFO and IDFC on the abundance of Bifidobacteriales and Lactobacillales at the order level (Fig. 3b, c). After 48 h of culture, DF, compared with the blank glucose (0.125), promoted the proliferation of Bifidobacteriales, and IDFC (0.625) was superior to IDFO (0.375), whereas DF, compared with blank glucose, promoted the abundance of Lactobacillales, and IDFO (7.25) was superior to IDFC (4.75). These results indicated differences in the utilization of the two DFs between Bifidobacteriales and Lactobacillales.

Similar findings have been found in other studies. Okara is consumed to a different extent by Lactobacilli and Bifidobacteria. There was no significant variation in okara uptake by *Lactobacillus acidophilus* after 24 h of incubation. Okara was not used for the first 48 h, whereas, its uptake increased significantly after 72 h and 96 h of fermentation (29.8% fermented substrate). These results indicated the high sensitivity of the changes in culture conditions and showed an adaptation of bifidobacteria to the okara substrate (Espinosa-Martos and Rupérez 2008). Similar findings have been found in previous studies. Whole Tibetan hull-less barley (WHB) was richer in DF than refined Tibetan hull-less barley (RHB). When WHB and RHB were fermented by human fecal bacteria in vitro, the IDF in WHB was used more than RHB. Next-generation sequencing of the bacterial 16S rRNA gene showed

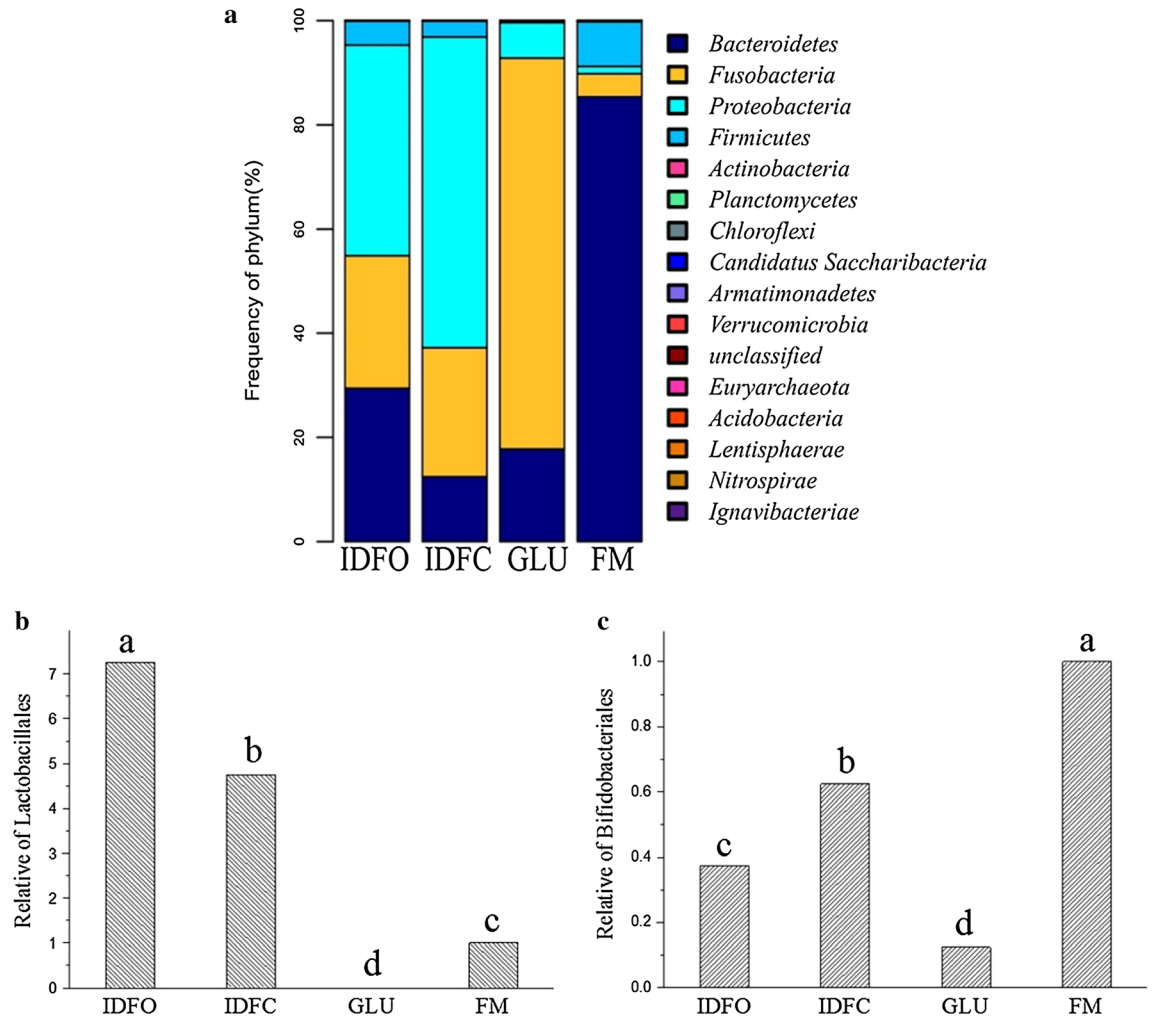

Fig. 3 Response of the fecal microbiota to DF treatment at the phylum level (**a**) and the effect of the abundance of Bifidobacteriales (**b**) and Lactobacillales (**c**) at the order level. *IDFO* insoluble dietary fiber from soy hull with oxalic acid extraction, *IDFC* insoluble dietary fiber from soy hull with citric acid extraction, *FM* fecal microflora, *GLU* glucose

that fermentation of both WHB and RHB significantly promoted the growth of *Bifidobacterium*; notably, the relative abundance of *Bifidobacterium* increased by 78.5% and 92.8%, compared with RHB and fructo-oligosaccharides, respectively, during WHB fermentation (Gong et al. et al. 2018a, b).

Conclusion

FTIR spectroscopy of IDFO and IDFC have no difference and have the same functional groups. IDFO has a sharp peak at 14.88°, whereas IDFC had a wider peak. IDFO included a compact regularly folded surface with visible attached particles and spherical substances, while IDFC formed a loose structure with a smooth surface, and the inner structure had holes exposed. Structural differences of IDFO and IDFC resulted in different physicochemical and functional properties. The moisture, protein, starch, ash, and SDF concentration of IDFC were higher than those of IDFO, whereas the fat and IDF concentrations were lower than those of IDFO. The WRC, WSC, and OAC of IDFC were greater than those of IDFO. The GAC, BRI, and α-AAIR of IDFC also were stronger than those of IDFO. Therefore, some differences of IDFO and IDFC at the micro-level resulted in collaboration between Bifidobacteriales and Lactobacillales to varying degrees. IDFC promoted the proliferation of Bifidobacteriales more than did IDFO, whereas IDFO promoted the abundance of Lactobacillales more than did IDFC. Thus this difference in regulating intestinal flora will provide a basis for further functional applications. This study provides theoretical knowledge for the research and utilization of SHDF.

Acknowledgements This study were supported by The National Natural Science Foundation of China (Nos. 31972031, 31901680). We thank International Science Editing for editing this manuscript.

Compliance with ethical standards

Conflict of interest The authors declare that they have no conflict of interest.

References

Abdul-Hamid A, Yu SL (2000) Functional properties of dietary fibre prepared from defatted rice bran. Food Chem 68(1):15–19

Ahmed F, Sairam S, Urooj A (2011) In vitro hypoglycemic effects of selected dietary fiber sources. J Food Sci Technol 48(3):285–289

Aljuraiban GS, Griep LM, Chan Q, Daviglus ML, Stamler J, Van Horn L, Frost GS (2015) Total, insoluble and soluble dietary fibre intake in relation to blood pressure: the INTERMAP study. Br J Nutr 114(9):1480–1486. https://doi.org/10.1017/S0007114515003098

Bibin Mathew C, Pothan LA, Tham NC, Günter M, Kottaisamy M, Sabu T (2008) A novel method for the synthesis of cellulose nanofibril whiskers from banana fibers and characterization. J Agric Food Chem 56(14):5617–5627

Chau C-F, Wang Y-T, Wen Y-L (2007) Different micronization methods significantly improve the functionality of carrot insoluble fibre. Food Chem 100(4):1402–1408. https://doi.org/10.1016/j.foodchem.2005.11.034

Chen Y, Ye R, Yin L, Zhang N (2014) Novel blasting extrusion processing improved the physicochemical properties of soluble dietary fiber from soybean residue and in vivo evaluation. J Food Eng 120(1):1–8

Clavel T, Lagkouvardos I, Hiergeist A (2016) Microbiome sequencing: challenges and opportunities for molecular medicine. Expert Rev Mol Diagn 16(7):795–805

Elleuch M, Bedigian D, Roiseux O, Besbes S, Blecker C, Attia H (2010) Dietary fibre and fibre-rich by-products of food processing: characterisation, technological functionality and commercial applications: a review. Food Chem 124(2):411–421

Espinosa-Martos I, Rupérez P (2008) Indigestible fraction of okara from soybean: composition, physicochemical properties and in vitro fermentability by pure cultures of *Lactobacillus acidophilus* and *Bifidobacterium bifidum*. Eur Food Res Technol 228(5):685–693. https://doi.org/10.1007/s00217-008-0979-7

Faith JJ, Guruge JL, Charbonneau M, Subramanian S, Seedorf H, Goodman AL, Leibel RL (2013) The long-term stability of the human gut microbiota. Science 341(6141):1237439

Figuerola F, Hurtado MAL, Estévez AMA, Chiffelle I, Asenjo F (2005) Fibre concentrates from apple pomace and citrus peel as potential fibre sources for food enrichment. Food Chem 91(3):395–401

Gong L, Cao W, Chi H, Wang J, Zhang H, Liu J, Sun B (2018a) Whole cereal grains and potential health effects: involvement of the gut microbiota. Food Res Int 103:84–102. https://doi.org/10.1016/j.foodres.2017.10.025

Gong L, Cao W, Gao J, Wang J, Zhang H, Sun B, Yin M (2018b) Whole tibetan hull-less barley exhibit stronger effect on promoting growth of genus *Bifidobacterium* than refined barley in vitro. J Food Sci 83(4):1116–1124. https://doi.org/10.1111/1750-3841.14086

Hashemi Z, Fouhse J, Im HS, Chan CB, Willing BP (2017) Dietary pea fiber supplementation improves glycemia and induces changes in the composition of gut microbiota, serum short chain fatty acid profile and expression of mucins in glucose intolerant rats. Nutrients. https://doi.org/10.3390/nu9111236

Kaczmarczyk MM, Miller MJ, Freund GG (2012) The health benefits of dietary fiber: beyond the usual suspects of type 2 diabetes mellitus, cardiovascular disease and colon cancer. Metabolism 61(8):1058–1066. https://doi.org/10.1016/j.metabol.2012.01.017

Kaushik A, Singh M (2011) Isolation and characterization of cellulose nanofibrils from wheat straw using steam explosion coupled with high shear homogenization. Carbohydr Res 346(1):76–85. https://doi.org/10.1016/j.carres.2010.10.020

Lam K-L, Ko K-C, Li X, Ke X, Cheng W-Y, Chen T, Cheung PC-K (2019) In vitro infant faecal fermentation of low viscosity barley β-glucan and its acid hydrolyzed derivatives: evaluation of their potential as novel prebiotics. Molecules 24(5):828

Lecumberri E, Mateos R, Izquierdo-Pulido M, Rupérez P, Goya L, Bravo L (2007) Dietary fibre composition, antioxidant capacity and physico-chemical properties of a fibre-rich product from cocoa (*Theobroma cacao* L.). Food Chem 104(3):948–954. https://doi.org/10.1016/j.foodchem.2006.12.054

Liu X, Wang J, Gu L, Yu HJ (2014) A preliminary study on extraction, isolation, purification and structure identification of Pleurotus Ostreatus Polysaccharides. J Mod Agric 3(3):42–48

Liu J, Hao Y, Wang Z, Ni F, Wang Y, Gong L, Wang J (2018) Identification, quantification, and anti-inflammatory activity of 5-n-Alkylresorcinols from 21 different wheat varieties. J Agric

Food Chem 66(35):9241–9247. https://doi.org/10.1021/acs.jafc.8b02911

López-Marcos MC, Bailina C, Viuda-Martos M, Pérez-Alvarez JA, Fernández-López J (2015) Properties of dietary fibers from agroindustrial coproducts as source for fiber-enriched foods. Food Bioprocess Technol 8(12):2400–2408. https://doi.org/10.1007/s11947-015-1591-z

Luo X, Wang Q, Fang D, Zhuang W, Chen C, Jiang W, Zheng Y (2018) Modification of insoluble dietary fibers from bamboo shoot shell: structural characterization and functional properties. Int J Biol Macromol 120:1461–1467

Ma MM, Mu TH (2016) Effects of extraction methods and particle size distribution on the structural, physicochemical, and functional properties of dietary fiber from deoiled cumin. Food Chem 194:237–246. https://doi.org/10.1016/j.foodchem.2015.07.095

Ma M, Mu T, Sun H, Zhang M, Chen J, Yan Z (2015) Optimization of extraction efficiency by shear emulsifying assisted enzymatic hydrolysis and functional properties of dietary fiber from deoiled cumin (*Cuminum cyminum* L.). Food Chem 179:270–277. https://doi.org/10.1016/j.foodchem.2015.01.136

McCleary BV, Sloane N, Draga A, Lazewska I (2013) Measurement of total dietary fiber using AOAC method 2009.01 (AACC International Approved Method 32-45.01): evaluation and updates. Cereal Chem J 90(4):396–414. https://doi.org/10.1094/cchem-10-12-0135-fi

Nishiyama Y, Langan P, Chanzy H (2003) Crystal structure and hydrogen-bonding system in cellulose Ibeta from synchrotron X-ray and neutron fiber diffraction. J Am Chem Soc 125(47):14300–14306

Qin J, Li R, Raes J, Arumugam M, Burgdorf KS, Manichanh C, Yamada T (2010) A human gut microbial gene catalogue established by metagenomic sequencing. Nature 464(7285):59

Rajilić-Stojanović M, de Vos WM (2014) The first 1000 cultured species of the human gastrointestinal microbiota. FEMS Microbiol Rev 38(5):996–1047

Sasaki D, Sasaki K, Ikuta N, Yasuda T, Fukuda I, Kondo A, Osawa R (2018) Low amounts of dietary fibre increase in vitro production of short-chain fatty acids without changing human colonic microbiota structure. Sci Rep 8(1):435. https://doi.org/10.1038/s41598-017-18877-8

Scheller HV, Ulvskov P (2010) Hemicelluloses. Annu Rev Plant Biol 61(1):263–289

Shang Q, Li Q, Zhang M, Song G, Shi J, Jiang H, Yu G (2016) Dietary keratan sulfate from shark cartilage modulates gut microbiota and increases the abundance of *Lactobacillus* spp. Mar Drugs. https://doi.org/10.3390/md14120224

Sowbhagya HB, Suma PF, Mahadevamma S, Tharanathan RN (2007) Spent residue from cumin—a potential source of dietary fiber. Food Chem 104(3):1220–1225. https://doi.org/10.1016/j.foodchem.2007.01.066

Strain CR, Collins KC, Naughton V, McSorley EM, Stanton C, Smyth TJ, Cherry P (2019) Effects of a polysaccharide-rich extract derived from Irish-sourced *Laminaria digitata* on the composition and metabolic activity of the human gut microbiota using an in vitro colonic model. Eur J Nutr. https://doi.org/10.1007/s00394-019-01909-6

Sun S-S, Wang K, Ma K, Bao L, Liu H-W (2019) An insoluble polysaccharide from the sclerotium of *Poria cocos* improves hyperglycemia, hyperlipidemia and hepatic steatosis in ob/ob mice via modulation of gut microbiota. Chin J Nat Med 17(1):3–14. https://doi.org/10.1016/s1875-5364(19)30003-2

Truchado P, Hernandez-Sanabria E, Salden BN, Van den Abbeele P, Vilchez-Vargas R, Jauregui R, Van de Wiele T (2017) Long chain arabinoxylans shift the mucosa-associated microbiota in the proximal colon of the simulator of the human intestinal microbial ecosystem (M-SHIME). J Funct Foods 32:226–237

Ullah I, Yin T, Xiong S, Huang Q, Zia ud D, Zhang J, Javaid AB (2018) Effects of thermal pre-treatment on physicochemical properties of nano-sized okara (soybean residue) insoluble dietary fiber prepared by wet media milling. J Food Eng 237:18–26. https://doi.org/10.1016/j.jfoodeng.2018.05.017

Velikonja A, Lipoglavsek L, Zorec M, Orel R, Avgustin G (2019) Alterations in gut microbiota composition and metabolic parameters after dietary intervention with barley beta glucans in patients with high risk for metabolic syndrome development. Anaerobe 55:67–77. https://doi.org/10.1016/j.anaerobe.2018.11.002

Vergara-Valencia N, Granados-Pérez E, Agama-Acevedo E, Tovar J, Ruales J, Bello-Pérez LA (2007) Fibre concentrate from mango fruit: characterization, associated antioxidant capacity and application as a bakery product ingredient. LWT—Food Sci Technol 40(4):722–729

Weickert MO, Roden M, Isken F, Hoffmann D, Nowotny P, Osterhoff M, Pfeiffer AF (2011) Effects of supplemented isoenergetic diets differing in cereal fiber and protein content on insulin sensitivity in overweight humans. Am J Clin Nutr 94(2):459–471. https://doi.org/10.3945/ajcn.110.004374

Wen Y, Niu M, Zhang B, Zhao S, Xiong S (2017) Structural characteristics and functional properties of rice bran dietary fiber modified by enzymatic and enzyme-micronization treatments. LWT 75:344–351. https://doi.org/10.1016/j.lwt.2016.09.012

Xiao M, Chery J, Keresztes I, Zax DB, Frey MW (2017) Direct characterization of cotton fabrics treated with di-epoxide by nuclear magnetic resonance. Carbohydr Polym 174:377–384. https://doi.org/10.1016/j.carbpol.2017.06.077

Yalegama LL, Nedra Karunaratne D, Sivakanesan R, Jayasekara C (2013) Chemical and functional properties of fibre concentrates obtained from by-products of coconut kernel. Food Chem 141(1):124–130. https://doi.org/10.1016/j.foodchem.2013.02.118

Yang J, Xiao A, Wang C (2014) Novel development and characterisation of dietary fibre from yellow soybean hulls. Food Chem 161:367–375. https://doi.org/10.1016/j.foodchem.2014.04.030